Supplementary Resources I:

Latest deep learning-based articles for EEG-based motor imagery classification

The content of this document is part of the following review paper:

Deep learning techniques for classification of electroencephalogram (EEG) motor imagery (MI) signals: a review

https://doi.org/10.1007/s00521-021-06352-5

For the details, the reader can refer to the above paper.

If you use the data in this document, please cite the original review paper as:

Altaheri, H., Muhammad, G., Alsulaiman, M. et al. Deep learning techniques for classification of electroencephalogram (EEG) motor imagery (MI) signals: a review. Neural Computing and Applications (2021). https://doi.org/10.1007/s00521-021-06352-5

Summary of the different deep learning models with the input formulation used for motor imagery (MI) classification

Deep Learning Model		Input Formulation: Extracted features: Temporal features: SM	NSCM	CorrM	PCA	Frequency features: DCT	FFT	PSD	Time-frequency features: EMD	HHT	WT	WPD	DWT	Spatial features: CSP	Spectral images: Time-frequency images (Generated by: E.g., WT, STFT, CWT, MW, ST, QTFD. Represented as: $[T \times F]^1$, $[T \times F \times C]^2$, $[T \times F+C]^3$ $[T+C \times F]^4$ $[(T+C) \times (F+C)]^5$): STFT	WT	MW	CWT	ST	QTFD	Spatial-frequency images (FFT energy map: $[C \times F]^1$, Energy: $[C \times F\text{-band}]^2$)	Raw signal values: 2D matrices (Segments of time-points) $[TP \times C]$ matrices	Topological maps: Time domain: Direct map: Time points (power values) 3D: [2D-map × Time]	Time Segments (average values): One map	Time Segments (average values): Multiple maps	Graph-based	Spectral domain (Generated by, e.g., CWT, ST, PSD, FFT): One map: ST	One map: CWT	One map: PSD	Multiple maps: FFT	Multiple maps: power
CNN			[81]	[66]		[75]		[76]	[9] [75]	[79]	[120]		[76]	[71] [72] [73] [143] [123] [126] [75] [82] [83]	[7]^{1} [90]^{3} [141]^{3} [92]^{3} [93]^{3} [98]^{3} [148]^{1} [130]^{2} [94]^{2}	[65]^{2}	[150]^{2}	[96]^{2} [97]^{4} [146]^{3} [147]^{3} [148]^{1}	[67]^{5}	[68]^{3}	[95]^{2} [89]^{1}	[103] [104] [105] [106] [107] [108] [62] [109] [135] [128] [110] [55] [129] [111] [127] [125] [121] [114] [112]^{A} [140] [57] [113] [122] [124]	[116] [117] [54]^{3D} [58]^{3D}		[118]		[67]	[119]	[119]	[118]	[118]
RNN	LSTM	[80]												[70] [84] [85]	[7]^{1} [90]^{3}																	
	GRU													[70]																		
ELM														[74]																		
DSN	DSN-RBM																				[149] [151]											
DBN	DBN-AE						[51]								[98]^{3}																	
	DBN-RBM				[86]		[51] [77]	[61]				[77] [78]		[78]																		
Hybrid	CNN+RNN														[7]^{1}																	
	CNN+GRU																						[59]									
	CNN+LSTM													[87] [88]							[137] [138] [63] [56]				[100]^{A}							
	CNN+AE														[98]^{3} [99]^{3VA}						[115] [60]											
	CNN+MLP																				[115]											
	CNN+GAN														[91]^{3}						[64]											
Generative	VAE														[91]^{3} [99]^{3}																	
	GAN														[91]^{3}						[64]											

A: Attention. Extracted features**,** ***SM****: Statistical measures,* ***CorrM****: Correlation matrix,* ***PCA****: Principal component analysis,* ***NSCM****: normalized sample covariance matrix.* Spatial features*,* ***CSP****: Common spatial pattern.* Frequency features*,* ***PSD****: Power spectral density,* ***FFT****: Fast Fourier transform,* ***DCT****: discrete cosine transform.* Time-frequency features*,* ***WT****: Wavelet transform,* ***DWT****: Discrete wavelet transform,* ***WPD****: Wavelet packet decomposition,* ***CWT****: Continuous wavelet transform,* ***MW****: Morlet wavelets,* ***STFT****: Short-time Fourier transform,* ***ST****: Stockwell Transform,* ***EMD****: Empirical mode decomposition,* ***HHT****: Hilbert-Huang transform,* ***QTFD****: quadratic time-frequency distribution,* ***ST****: Stockwell transform.* Image representation*, (For details, refer to Figure 10),* ***T****: Time window (time segment),* ***TP****: Time point (sampling point),* ***F****: Frequency,* ***F-band****: Frequency band,* ***C****: Channel (electrode).* Deep Learning Models*,* ***CNN****: Convolutional neural network,* ***RNN*** *Recurrent neural network,* ***LSTM****: Long short-term memory,* ***GRU****: Gated recurrent unit,* ***MLP****: Multi-layer perceptron,* ***AE****: Auto-encoder,* ***RBM****: Restricted Boltzmann machine,* ***DBN****: Deep belief network,* ***GAN****: Generative adversarial network,* ***VAE****: Variational autoencoder,* ***ELM****: Extreme learning machine,* ***DSN****: Deep stacking network,*

Summary of artifact removal strategies used for MI-EEG signals

Artifacts removal approach									
AR: Automatic removal							Manual removal	Without removal	Not specified
ICA	BSS+MRIC	DWT	ASR	AAR	Others (E.g., SW such as BCILAB or EEGLAB)	SF: CAR			
[7] [62] [63] [64]	[147]	[97]	[64]	[68] [66]	[71] [61] [9] [76] [120] [78]	[65] [66] [67] [60]	[116] [137] [126]	[103] [98] [104] [115] [105] [70] [77] [99] [100] [141] [91] [93] [109] [143] [51] [54] [84] [149] [123] [130] [150] [151] [110] [85] [58] [129] [111] [127] [125] [121] [114] [59] [112] [57] [113]	[90] [106] [118] [72] [74] [117] [95] [92] [96] [138] [107] [108] [79] [89] [73] [86] [119] [80] [56] [146] [87] [148] [135] [75] [128] [55] [81] [88] [82] [94] [140] [83]

***ICA**: Independent component analysis, **DWT**: Discrete wavelet transform, **SF:** Spatial filter, **CAR**: Common average reference filter, **AAR**: Automatic artifact removal, **ASR**: Artifact subspace reconstruction, **BSS**: Blind Source Separation, **MRIC**: Movement Related Independent Component, **SW**: software.*

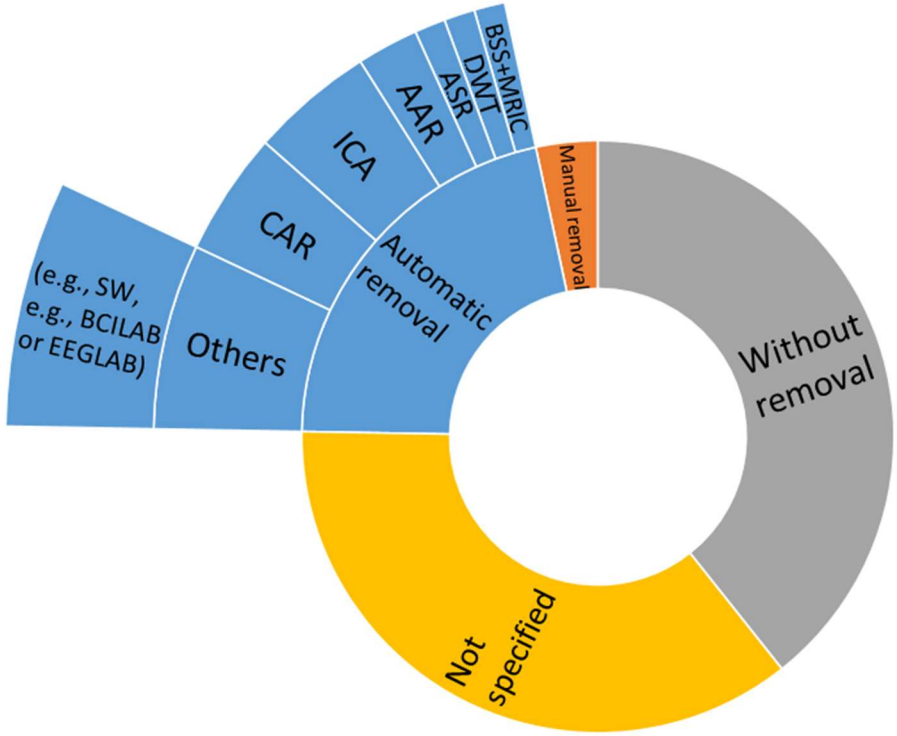

Summary of the latest deep learning-based articles for EEG-based motor imagery classification.

Study	Pre-processing			Input formulation*	Deep learning approaches			Dataset	Performance evaluations			
	Selected channels	Analyzed frequency band (Hz)	Artifact removal approach		General strategy	Architecture	Activation function		Strategy	Performance measures		
										Accuracy %	kappa	Others (name)
Zhang et al. 2021, [128]	ALL (62)	8-30	N/A	RV: 2D matrices [TP × C]	CNN (adaptive transfer learn.)	5 CONV 1 FC 2 OUT	ELU: conv Smax: L-FC	Lee et al. [50]	sub-d: HO (70: 30) sub-i: CV (LOSO)	sub-d: 63.54±14.25 sub-i: 84.19±9.98	–	Computation time, t-test
Zhang et al. 2021, [114]	ALL (22, 3)	FB (0.5-100)	W	RV: 2D matrices [TP × C]	CNN (inception) (augment: NS)	6×5 CONV 2 FC 4/2 OUT	ReLU: conv N/A: FC Smax: L-FC	DS1: BCI-C IV-2a [131] DS2: BCI-C IV-2b [101]	HO (75 : 25)	DS1: 88.4±7 DS2: 88.6±5	–	CM, ROC, AUC, F-score, TPR
Avilov et al. 2021, [55]	variable (3-128)	4-38	N/A	RV: 2D matrices [TP × C]	CNN	3 CONV 1 FC 2 OUT	ELU: conv Smax: L-FC	Local: 22 sub, 2 MI (presses/releases a button), 128 elec, 1144 trials/class, 2048 Hz.	CV (10 folds)	83.2	–	–
Kumar et al. 2021, [85]	ALL (64)	Adaptive selection	W	EF: CSP	RNN-LSTM +SVM	2 LSTM-L 1 FC 2 OUT	N/A	GigaDB [132]	CV (10 folds)	69.59	0.398	TPR, TNR
Liu et al. 2021, [58]	ALL (22) +variable	FB (0.5-100)	W	TM: TP-3D	CNN (3D) (residual) (multi-branch)	10 CONV 3 FC 4 OUT	ELU: conv ReLU: FC Smax: L-FC	BCI-C IV-2a [131]	CV (10 folds)	81.22 ± 6.85	0.72 ± 0.12	p-value, test/train time
Zhao et al. 2021, [129]	ALL (22, 3)	4-38	W	RV: 2D matrices [TP × C]	CNN (domain adaptation)	2 CONV 3 FC 4/2 OUT	ReLU: conv ReLU: FC sigm: L-FC	DS1: BCI-C IV-2a [131] DS2: BCI-C IV-2b [101]	c-sub: HO DS1: (50:50) DS2: (56:44)	DS1: 74.75 DS2: 83.98	DS1: 0.663 DS2: 0.68	–
Bang et al. 2021, [81]	DS1: 22 DS2: 3 DS3: 20	4-40	N/A	EF: NSCM	CNN (3D)	2 CONV 2 FC 2 OUT	ReLU: conv ReLU: FC N/A: L-FC	DS1: BCI-C IV-2a [131] DS2: BCI-C IV-2b [101] DS3: Lee et al. [50]	CV (10 folds)	DS1: 87.15 DS2: 75.85 DS3: 70.37	–	t-test
Deng et al. 2021, [103]	ALL (22, 60)	4-38	W	RV: 2D matrices [TP × C]	CNN	3 CONV 1 FC 4 OUT	ELU: conv Smax: L-FC	DS1: BCI-C IV-2a [131] DS2: BCI-C III-3a [136]	CV (5 folds)	DS1: 78.96 DS2: 85.30	DS1: 0.72 DS2: 0.80	t-test
Ha et al. 2021, [127]	ALL (22, 3)	4-38	W	RV: 2D matrices [TP × C]	CNN (multi-level pooling)	4 CONV 2 FC 4/2 OUT	ELU: conv ELU: FC Smax: L-FC	DS1: BCI-C IV-2a [131] DS2: BCI-C IV-2b [101]	HO DS1: (50:50) DS2: (56:44)	DS1: 73.19 DS2: 82.83	–	w-test
Zhang et al. 2021, [88]	ALL (22)	4-40	N/A	EF: CSP	Hybrid: CNN/LSTM (transfer learn.)	3 CONV 1 LSTM-L 4 FC 4 OUT	ReLU: conv ReLU: FC Smax: L-FC	BCI-C IV-2b [101]	c-sub: HO (50 : 50)	–	0.81	–
Riyad et al. 2020, [125]	ALL (22)	0-38 4-38	W	RV: 2D matrices [TP × C]	CNN (inception) (augment: SW)	11 CONV 1 FC 4 OUT	ELU: conv Smax: L-FC	BCI-C IV-2b [101]	CV (5 folds)	74.61	0.662	CM
Liu et al. 2020, [121]	ALL (22)	0-38	W	RV: 2D matrices [TP × C]	CNN (self-attention) (transfer learn.)	7 CONV 1 FC 4 OUT	N/A: conv Smax: L-FC	BCI-C IV-2b [101]	c-sub: CV (10 folds) HO (50 : 50)	HO: 78.51 CV: 90.15	–	CM
Xue et al. 2020, [82]	ALL (22, 60)	4-40	N/A	EF: CSP	CNN (multi-layer)	7 CONV 3 FC 4 OUT	ELU: conv ELU: FC Smax: L-FC	DS1: BCI-C IV-2b [101] DS2: BCI-C III-3a [136]	HO (70 : 30)	DS1: 83.83 DS2: 89.45	DS1: 0.78 DS2: 0.86	–
Li et al. 2020, [106]	ALL (22)	8-30	W	RV: 2D matrices [TP × C]	CNN (multi-scale) (attention)	10 CONV 2 FC 4 OUT	ReLU: conv ReLU: FC Smax: L-FC	BCI-C IV-2b [101]	HO (50 : 50)	79.9	–	CM
Li et al. 2020, [59]	ALL (64) +variable	N/A	W	TM: TP (D)	Hybrid: CNN/GRU	3 CONV 1 FC 2 GRU-L 2 FC 4 OUT	N/A: conv N/A: FC Smax: L-FC	EEGMMIDB [139]	HO (75 : 25)	97.36	–	–
Fan et al. 2020, [104]	ALL (64)	0.1-64	W	RV: 2D matrices [TP × C]	CNN (attention) (residual)	14 CONV 1 FC 4 OUT	ReLU: conv N/A: L-FC	EEGMMIDB [139]	CV (5 folds)	65.82	–	CM
Roy et al. 2020, [94]	ALL (3)	4-32	N/A	SI: TFI (STFT) [T × F × C]	CNN	3 CONV 2 FC 2 OUT	ReLU: conv N/A: FC Smax: L-FC	BCI-C IV-2b [101]	sub-d: HO (56 : 44) sub-i: CV (LOSO)	sub-d: 77.5±14.5 sub-i: 70.9±9.9	sub-d: 0.55±0.29 sub-i: 0.42±0.2	–
Xiaoling et al. 2020, [140]	28	8-30	N/A	RV: 2D matrices [TP × C]	CNN	2 CONV 2 FC 2 OUT	tanh: conv sigm: FC sigm: L-FC	Local: 4 sub, 2 MI left-hand/foot, 560 trials/sub, 1000 Hz (1-40 Hz), 64 elec.	HO (80 : 20)	90.08±2.22	–	CM, RC, PR, F-score, ROC, w-test, T-comp
Lun et al. 2020, [57]	2 +variable	N/A	W	RV: 2D matrices [TP × C]	CNN	5 CONV 1 FC 4 OUT	LReLU: conv Smax: L-FC	EEGMMIDB [139]	sub-d: CV (10 folds) sub-i: HO (106: 3 subs)	sub-d: 94.80 sub-i: 72.47	–	CM, RC, PR, F-score, ROC, AUC
Roots et al. 2020, [105]	ALL (64)	2-60	W	RV: 2D matrices [TP × C]	CNN (multi-branch) (augment: SW)	3×3 CONV 1 FC 2 OUT	ELU: conv Smax: L-FC	EEGMMIDB [139]	c-sub HO (80 : 20)	83.8	–	CM, RC, PR, F-score, t-test
Yang et al. 2020, [60]	variable (3-25)	7-35	A: CAR	RV: 2D matrices [TP × C]	Hybrid: CNN/SAE (multi-layer-CNN)	5 CONV 2 AE (1 hid) 1 FC 2 OUT	ReLU: conv Smax: L-FC	DS1: BCI-C IV-1 [133] DS2 (Local): 6 sub, 2 MI L/R hand, 64 elec, 300 trials/sub, 256 Hz.	sub-d: CV (8 folds) sub-i: CV (LOSO)	sub-i: DS1: 86.4 DS2: 84.7	sub-i DS1: 0.45 DS2: 0.46	–
Zhao et al. 2020, [83]	ALL (64, 22)	4-40	N/A	EF: CSP	CNN (domain adaptation)	4 CONV 1 FC 2 OUT	ReLU: conv Smax: L-FC	DS1: GigaDB [132] DS2: BCI-C IV-2a [131]	c-sub: HO (8 : 1 subs) (5 : 1 subs)	N/A	–	–
Zhang et al. 2020, [100]	ALL (64, 22)	FB (DS2: 0.5-100)	W	TM: TP (G)	Hybrid: CNN/LSTM (recurrent attention)	1 CONV 2 LSTM-L 1 FC 4 OUT	ELU: conv Smax: L-FC	DS1: EEGMMIDB [139] DS2: BCI-C IV-2a [131]	sub-i: HO (subs) DS1: (95:10) DS2: (8 : 1)	DS1: 74.2 DS2: 60.1	–	ROC, AUC
Xu et al. 2020, [116]	ALL (22)	9-20 +variable	M	TM: TP (D)	CNN	3 CONV 2 FC 4 OUT	ReLU: conv ReLU: FC Smax: L-FC	BCI-C IV-2a [131]	HO	84.57	0.801	–
Zhang et al. 2020, [141]	ALL (3)	8-30	W	SI: TFI (STFT) [T× F+C]	CNN	2 CONV 2 FC 2 OUT	ReLU: conv Smax: FC Smax: L-FC	BCI-C IV-2b [101]	CV (10 folds)	94.7 ± 2:6	0.664	–
Liao et al. 2020, [117]	ALL (22)	4-40	N/A	TM: TP (D)	CNN	3 CONV 1 FC 4 OUT	LReLU: conv Smax: L-FC	BCI-C IV-2a [131]	HO (50 : 50)	74.60	0.66	–

Zhang et al. 2020, [91]	3	8-30	W	SI: TFI (STFT) [T × F+C]	Hybrid: CNN/GAN (also VAE)	4:4 CONV CNN: 2 CONV 2 FC 2 OUT	LReLU: d-conv ReLU: conv Smax: FC Smax: L-FC	DS1: BCI-C IV-1 [133] DS2: BCI-C IV-2b [101]	CV (10 folds)	DS1: 83.2 ± 3.5 DS2: 93.2 ± 2.8	DS1: 0.468 DS2: 0.671	t-test, p-value
Miao et al. 2020, [95]	49	8–30	N/A	SI: SFI (Energy) [C × F-band]	CNN	2 CONV 3 FC 2 OUT	ReLU: conv ReLU: FC Smax: L-FC	DS1: BCI-C III-4a [136] DS2 (Local): 5 sub, 2 MI finger/rest, 21 elec, 1000 Hz.	CV (10 folds)	DS1: 90.0	–	Running time
Tang et al. 2020, [9]	3	8–30	A	EF: (EMD)	CNN (1D) (multi-scale) (inception)	4 CONV 2 FC 2 OUT	ReLU: conv N/A: FC Smax: L-FC	DS1: BCI-C IV-2b [101] DS2 (Local): 5 sub, 2 MI L/R hand, 14 elec, 128 Hz, 10 s trial.	N/A	DS1: 82.61 DS2: 85.83	–	p-value
Shajil et al. 2020, [92]	5	1-100 13-30	N/A	SI: TFI (STFT) [T× F+C]	CNN	1 CONV 2 FC 4 OUT	ReLU: conv N/A: FC Smax: L-FC	Local: 12 sub, 4 MI (L/R hand, both hands, feet), 16 elec, 500 Hz.	N/A	87.37 ± 1.68	–	–
Xu et al. 2020, [78]	ALL (22)	8-30	A: EEGLAB	EF: WPD, CSP	DBN-RBM (stacked RBM) +SVM	4 RBM (1 hid) 4 OUT	sigm: RBM Linear: last RBM	BCI-C IV-2a [131]	CV (10 folds)	78.51	0.6278	–
Taheri et al. 2020, [75]	1	N/A	N/A	EF: CSP, DCT, EMD	CNN+SVM (multi-branch)	5 CONV 2 FC 2 OUT	ReLU: conv ReLU: FC	BCI-C III-4a [136]	HO (70 : 30)	96.34	–	–
Wang et al. 2020, [137]	ALL (22)	8-30	M	RV: 2D matrices [TP × C]	Hybrid: CNN/LSTM	3 CONV 1 FC 2 LSTM-L 1 FC 4 OUT	ELU/Linaer: conv Smax: L-FC	BCI-C IV-2a [131]	HO (50 : 50)	–	0.64 ± 0.14	t-test
Li et al. 2020, [96]	ALL (3)	4-30	N/A	SI: TFI (CWT) [T×F×C]	CNN	2 CONV 2 FC 2 OUT	ReLU: conv ReLU: FC Smax: L-FC	BCI-C IV-2b [101]	CV (10 folds)	83.2	0.651	–
Rong et al. 2020, [93]	ALL (3)	4-32	W	SI: TFI (STFT) [T× F+C]	CNN	3 CONV 1 FC 2 OUT	ReLU: conv Smax: L-FC	BCI-C IV-2b [101]	HO (90 : 10)	82.8	0.663	–
Ma et al. 2020, [76]	ALL (22)	0.5-50	A	EF: DWT +PSD	CNN	4 CONV 2 FC 4 OUT	ReLU: conv N/A: FC N/A: L-FC	BCI-C IV-2a [131]	CV (8 folds)	96.21	–	test/train time
Hou et al. 2020, [120]	ALL (64)	8-30	A	EF: WT	CNN	6 CONV 2 FC 4 OUT	LReLU: conv LReLU: FC Smax: L-FC	EEGMMIDB [139]	CV (10 folds)	94.5	–	–
Freer et al. 2020, [138]	ALL (22)	7-30	N/A	N/A	Hybrid: CNN/LSTM (augment)	4 CONV 1 LSTM-L 1 FC 4 OUT	ELU: conv Smax: L-FC	BCI-C IV-2a [131]	N/A	–	–	PR, RC
Dai et al. 2020, [111]	3	4-32	N/A	RV: 2D matrices [TP × C]	CNN (multi-layer) (augment)	2 CONV 2 FC 4/2 OUT	ELU: conv N/A: FC N/A: L-FC	DS1: BCI-C IV-2a [131] DS2: BCI-C IV-2b [101]	HO	DS1: 91.57 DS2: 87.6	–	P-values
Lee et al. 2020, [112]	24	4-40	N/A	RV: 2D matrices [TP × C]	CNN (multi-branch)	4 CONV 1 FC 9 OUT	ELU: conv Smax: L-FC	Local: 9 MI, 12 sub, 50 trials/sess, 3 sess, 1000 Hz, 64 elec.	CV (5 folds)	81	–	CM
Huang et al. 2020, [79]	ALL (22)	FB 0.5-100	N/A	EF: HHT	CNN	5 CONV 2 FC 4 OUT	Linear/ReLU: conv N/A: FC Smax: L-FC	BCI-C IV-2a [131]	CV (4 folds)	77.9	–	–
Li et al. 2020, [118]	ALL (64, 22, 3)	8-30	N/A	TM: TP (D)	CNN	31 CONV 1 FC 4/4/2 OUT	ReLU: conv Smax: L-FC	DS1: EEGMMIDB [139] DS2: BCI-C IV-2a [131] DS3: BCI-C IV-2b [101]	DS1,3: CV (10 folds) DS2: HO (50 : 50)	DS1,CV: 89 DS2,HO: 89 DS3,CV: 97	DS1: 0.77 DS2: 0.78 DS3: 0.94	CM, ROC, AUC
Alwasiti et al. 2020, [67]	ALL (64)	2-78	A: CAR	SI: ST [T+C × F+C]	CNN (DenseNet) (deep metric learning)	1 CONV 4 DB 2 FC 3 OUT	ReLU: conv ReLU: DB ReLU: FC Smax: L-FC	EEGMMIDB [139]	HO (80 : 20)	64.7	–	CM, PR, RC
Jeong et al. 2020, [62]	20	4-40	A: ICA	RV: 2D matrices [TP × C]	CNN (multi-layer)	5 CONV 2 FC 3 OUT	ELU: conv ELU: FC Smax: L-FC	DS1: ULMov [142] DS2 (Local): 10 sub, 3 MI (forearm angle), 150 trials, 100 Hz, 32 elec.	HO (80 : 20)	DS1: 51.0 ± 4.0 DS2: 65.0 ± 9.0	–	CM, t-test
Cheng et al. 2020, [86]	ALL	0.5-30	N/A	EF: PCA	DBN-RBM	5 RBM (1 hid) 1 FC 2 OUT	Smax: L-FC	DS1: BCI-C IV-2b [101] DS2: BCI-C II-3 [102]	CV (10 folds)	DS1: 91.71 DS2: 96.25	DS1: 0.8342 DS2: 0.925	t-test, test/train time
Collazos et al. 2020, [119]	ALL (22)	8-30	N/A	TM: SP (CWT, PSD)	CNN (multiple input CNN)	4 CONV 2 FC 3 OUT	ReLU: conv ReLU: FC Smax: L-FC	BCI-C IV-2a [131]	CV (10 folds)	71.2 ± 7.0	0.56	p-values
Chen et al. 2020, [143]	ALL (22, 15)	8-30	W	EF: CSP	CNN	3 CONV 2 FC 4 OUT	ReLU: conv N/A: FC Smax: L-FC	DS1: BCI-C IV-2a [131] DS2: Steyrl et al. [144]	HO (70 : 30)	DS1: 72 DS2: 82.9	DS1: 0.627 DS2: 0.657	CM, t-test
Kant et al. 2020, [97]	ALL (2)	8-30	A: DWT	SI: TFI (CWT) [T+C ×F]	CNN (transfer learning)	14 CONV 4 FC 2 OUT	ReLU: conv ReLU: FC Smax: L-FC	BCI-C II-3 [102]	HO (50 : 50)	95.71	0.91	CM
Fahimi et al. 2020, [64]	ALL	0.5-100	A: ICA, ASR	RV: 2D matrices [TP × C]	Hybrid: CNN/GAN	2:2 CONV 3 CONV 2 FC 2 OUT	tanh: G-conv ReLU: conv ReLU: FC sigm: L-FC	DS1: BCI-C III-4a [136] DS2 (Local): 14 sub, 2 MI open/close R-hand, 62 elec.	HO (50 : 50)	DS1: 71.14	–	–
Ma et al. 2019, [66]	ALL (64)	0.1-40	A: CAR, AAR	EF: CorrM	CNN (multi-branch)	2 CONV 1 FC 3 OUT	ReLU: conv Smax: L-FC	MIJoint [145]	CV (5 folds)	87.03	–	–
Hassanpour et al. 2019, [51]	ALL (22) +variable	8-35	W (+A: SWT)	EF: FFT	DBN-AE DBN-RBM (augment: SW)	5 RBM/AE (1 hid) 1 FC 4 OUT	N/A: AE Smax: L-FC	BCI-C IV-2a [131]	HO (50 : 50)	DBN-AE: 71.0 DBN-RBM: 68.4	–	t-test, train time
Zhu et al. 2019, [56]	variable (3-64)	N/A	N/A	RV: 2D matrices [TP × C]	Hybrid: CNN/LSTM (also CNN)	2 CONV 1 LSTM-L 1 FC 2 OUT	N/A	EEGMMIDB [139]	N/A	82.93 (CNN: 79.7)	–	–
Lee et al. 2019, [146]	ALL (3)	8-30	N/A	SI: TFI (CWT) [T× C+F]	CNN	1 CONV 1 FC 2 OUT	ReLU: conv N/A: L-FC	DS1: BCI-C IV-2b [101] DS2: BCI-C II-3 [102]	CV (10 folds)	DS1: 83.0±1.6 DS2: 92.9	–	–
Zhang et al. 2019, [87]	ALL (22)	4-38	N/A	EF: FBCSP	Hybrid: CNN/LSTM	3 CONV 3 LSTM-L 4 OUT	ReLU: conv Smax: out	BCI-C IV-2a [131]	HO	84	0.81	–

Amin et al. 2019, [115]	ALL (22)	0.5-40	W	RV: 2D matrices [TP × C]	Hybrid: CNN/MLP (M) CNN/AE (A) (multi-layer-CNN)	5 CONV 4 FC MLP (2 hid)/ AE (1 hid) 4 OUT	ELU: conv ELU: AE ELU: MLP N/A: FC Smax: L-FC	BCI-C IV-2a [131]	sub-d: HO (50 : 50) sub-i: CV (LOSO)	sub-d: M: 75, A: 73 sub-i: M: 42, A: 55	–	CM, train time
Wu et al. 2019, [113]	ALL (22, 3)	4-38	W	RV: 2D matrices [TP × C]	CNN	5 CONV 1 FC 4/2/3 OUT	Linear	DS1: BCI-C IV-2a [131] DS2: BCI-C IV-2b [101]	c-sub: HO	DS1: 75.9 DS2: 84.7	–	–
Ortiz et al. 2019, [147]	18	0.5-90	A: BSS+ MRIC	SI: CWT [T × C+F]	CNN	2 CONV 2 FC 2 OUT	ReLU: conv ReLU: FC Smax: L-FC	BCI-C III-4a [136]	CV (10 folds)	94.66	–	–
Zhao et al. 2019, [54]	ALL (22) +variable	0.5-100 +variable	W	TM: TP-3D	CNN (3D) (multi-branch)	3 CONV 3 FC 4 OUT	ELU: conv ReLU: FC Smax: L-FC	BCI-C IV-2a [131]	CV (10 folds)	75.02	0.644	t-test, test/train time
Kumar et al. 2019, [84]	ALL (64, 59)	7-30	W	EF: CSP	RNN-LSTM	2 LSTM-L 1 FC 2 OUT	N/A	DS1: GigaDB [132] DS2: BCI-C IV-1 [133]	CV (10 folds)	DS1: 68.19 DS2: 82.52	DS1: 0.374 DS2: 0.650	TPR, TNR
Chaudhary et al. 2019, [148]	N/A	N/A	N/A	SI: TFI (STFT/CWT) [T × F]	CNN	5 CONV 3 FC 2 OUT	ReLU: conv Smax: FC Smax: L-FC	BCI-C III-4a [136]	HO (80 : 20)	99.35	0.987	TPR, TNR, F-score, CM
Li et al. 2019, [135]	ALL (22)	N/A	N/A	RV: 2D matrices [TP × C]	CNN (augment: AP)	5 CONV 2 FC 4 OUT	ELU: conv ELU: FC Smax: L-FC	BCI-C IV-2a [131]	HO (50 : 50)	74.6	–	CM, PR, RC, F-score, train time
Tang et al. 2019, [149]	DS1: ALL (3) DS2: 6	8-30	W	RV: 2D matrices [TP × C]	DSN-RBM (semi-supervised)	7 RBM (1 hid) 2 OUT	N/A	DS1: BCI-C IV-2b [101] DS2 (Local): 7 sub, 2 MI L/R hand, 128 Hz, 240 trials/sub, 14 elec.	HO	DS1: 83.55	–	p-value, train time
Zhu et al. 2019, [123]	ALL (3, 15)	8-30	W	EF: CSP	CNN (residual)	13 CONV 1 FC 2 OUT	ReLU: conv Smax: L-FC	DS1: BCI-C IV-2b [101] DS2 (Local): 25 sub, 2 MI L/R hand, 1000 Hz, 200 trials/sub, 15 elec.	sub-i CV (LOSO)	DS1: 64.0 DS2: 73.0	–	ITR
Dai et al. 2019, [99]	ALL (3, 5)	6-30	W	SI: TFI (STFT) [T × F+C]	Hybrid: CNN/VAE	1 CONV 5 hid. VAE 2 OUT	ReLU: conv	DS1: BCI-C IV-2b [101] DS2 (Local): 5 sub, 2 MI L/R hand, 400 trials, 3 sess, 250 Hz, 5 elec.	CV (10 folds)	–	DS1: 0.564 DS2: 0.568	p-value, train time
Olivas-Padilla et al. 2019, [71]	8	8-30	A: BCIL AB	EF: FBCSP (set as a matrix)	CNN	4 CONV 1 FC 4 OUT	ReLU: conv Smax: L-FC	DS1: BCI-C IV-2a [131] DS2 (Local): 8 sub, 4 MI L/R hand/foot, 5 sess, 120 trials/sess, 250 Hz, 8 elec.	DS1: HO (50 : 50) DS2: CV (10 folds)	DS1: 78.41±5.9 DS2: 73.78±4.2	DS1: 0.59±0.11 DS2: 0.64±0.07	–
Alazrai et al. 2019, [68]	ALL (16)	0.5-32.5	A: AAR	SI: TFI (QTFD) [T× F+C]	CNN+SVM	2 CONV 1 FC 11 OUT	ReLU: conv Smax: L-FC	Local: 11 MI, 22 sub, 2048 Hz, 16 elec.	CV (10 folds)	73.70	–	PR, RC, F-score, train/test time
Li et al. 2019, [126]	ALL (22)	8-30	M	EF: CSP	CNN (multi-layer)	9 CONV 2 FC 4 OUT	ReLU: conv Smax: FC Smax: L-FC	BCI-C IV-2a [131]	HO (50 : 50)	79.9	–	–
Xu et al. 2019, [130]	ALL (3)	4-32	W	SI: TFI (STFT) [T×F×C]	CNN (transfer learning)	13 CONV 3 FC 2 OUT	ReLU: conv ReLU: FC Smax: L-FC	BCI-C IV-2b [101]	HO (80 : 20)	74.2	–	train time
Zhang et al. 2019, [150]	ALL (3, 14)	8-30	W	SI: TFI (WT: MW) [T×F×C]	CNN (augment)	2 CONV 2 FC 2 OUT	ReLU: conv ReLU: FC Smax: L-FC	DS1: BCI-C II-3 [102] DS2 (Local): 5 sub, 2 MI L/R hand, 256 Hz, 120 trials/sub, 14 elec.	CV (5 folds)	DS1: 90.1 DS2: 90.0	–	–
Amin et al. 2019, [108]	ALL (22)	FB (0.5-100)	W	RV: 2D matrices [TP × C]	CNN (multi-layer)	5 CONV 4 FC 1 FC 4 OUT	ELU: conv ELU: FC Smax: L-FC	BCI-C IV-2a [131]	sub-i: CV (LOSO)	74.5	–	CM, PR, RC, train time
Tayeb et al. 2019, [7]	ALL (3)	2-60	A: ICA (FASTER)	SI: TFI (STEF) [T × F]	CNN (also LSTM, and RCNN (CNN\RNN))	3 CONV 1 FC 2 OUT	ReLU: conv Smax: L-FC	DS1: BCI-C IV-2b [101] DS2 (Local-public): 20 sub, 2 MI L/R hand, 2 sess, 4 runs, total 750 trials, 256 Hz, 3 elec.	CV (5 folds)	DS1: CNN: 91.63 DS2: CNN: 84.24 RCNN: 77.7	–	–
Kwon et al. 2019, [73]	20	0-40	N/A	EF: CSP	CNN (multi-branch)	3×3 CONV 2 FC 2 OUT	ReLU: conv N/A: FC Smax: L-FC	Lee et al. [50]	sub-d: HO (50 : 50) sub-i: CV (LOSO)	sub-d: 71.3±15.8 sub-i: 74.2±15.8	–	t-test
Xu et al. 2018, [65]	DS1: 3 (DS2:ALL)	8-30	A: CAR	SI: TFI (WT) [T×F×C]	CNN	2 CONV 2 FC 4/2 OUT	ReLU: conv N/A: FC N/A: L-FC	DS1: BCI-C IV-2a [131] DS2: BCI-C II-3 [102]	CV (5 folds)	DS1: 85.59 DS2: 89.56	DS1: 0.766	F-score, train time
She et al. 2018, [74]	ALL (22)	8-30	N/A	EF: CSP	ELM	3 hid 2 OUT	N/A	BCI-C IV-2a [131]	CV (9 folds)	67.76	0.5701	–
Dose et al. 2018, [109]	ALL (64)	N/A	W	RV: 2D matrices [TP × C]	CNN	2 CONV 1 FC 2/3/4 OUT	ReLU: conv Smax: L-FC	EEGMMIDB [139]	CV (5 folds)	2-class: 80.4 3-class:69.8 4-class:58.6	–	CM, PR, RE, train time
Wang et al. 2018, [90]	3	8-30	N/A	SI: TFI (STFT) [T× F+C]	CNN (also LSTM)	2 CONV 2 FC 2 OUT	SELU: conv N/A: FC Smax: L-FC	Local: 14 sub, 2 MI L/R hand, 60 trials/sub, 256 Hz, 11 elec.	CV (4 folds)	CNN: 92.73 LSTM: 80.2	–	CM, p-value
Sakhavi et al. 2018, [72]	ALL (22)	4-40	N/A	EF: CSP	CNN	3 CONV 1 FC 4 OUT	ReLU: conv Smax: L-FC	BCI-C IV-2a [131]	CV (10 folds)	74.46	0.659	–
Wang et al. 2018, [80]	ALL (22)	FB (0.5-100)	N/A	EF: SM	RNN-LSTM	3 LSTM-L 2 OUT	N/A	BCI-C IV-2a [131]	CV (5 folds)	79.6	–	–
Lawhern et al. 2018, [107]	ALL (22)	4-40	W	RV: 2D matrices [TP × C]	CNN	3 CONV 1 FC 4 OUT	ELU: conv Smax: L-FC	BCI-C IV-2a [131] (128 samples/s)	CV (4 folds)	69	–	AUC
Luo et al. 2018, [70]	ALL (22, 3)	8-30	W	EF: FBCSP (time slices)	RNN-GRU (also RNN-LSTM)	2 GRU-L/ LSTM-L 1 FC 4/2 OUT	N/A	DS1: BCI-C IV-2a [131] DS2: BCI-C IV-2b [101]	HO DS1: (50:50) DS2: (56:44)	GRU: 73.6, 82.8 LSTM: 72.6, 81.5	–	train/test time, complexity, t-test
Chu et al. 2018, [61]	ALL (64)	FB (8-35)	A	EF: PSD (LSP)	DBN-RBM	3 RBM (1 hid) 1 FC 3 OUT	Smax: L-FC	Local: 9 sub, 3 MI L/R hand and foot, 10 runs, 300 trials/sub, 10 s trial, 1000 Hz, 64 elec.	HO (75 : 25)	70.72 ± 2.68	–	–

Yang et al. 2018, [63]	9	N/A	A: ICA	RV: 2D matrices [TP × C]	Hybrid: CNN/LSTM	3 CONV 1 LSTM-L 1 FC 2 OUT	ReLU: conv Smax: L-FC	Local: 2 MI L hand/R foot, 6 sub, 500 Hz, 9 elec.	HO (70 : 30)	86.7	–	ROC, train time
Tang et al. 2017, [151]	DS1: ALL(3) DS2: 6	8-30	W	RV: 2D matrices [TP × C]	DSN-RBM	2 RBM (1 hid) 2 OUT	N/A	DS1: BCI-C IV-2b [101] DS2 (Local): 7 sub, 2 MI L/R hand, 128 Hz, 240 trials/sub, 14 elec.	HO (50 : 50)	DS1: 81.35	–	p-value
Tang et al. 2017, [110]	ALL (28)	8-30	N/A	RV: 2D matrices [TP × C]	CNN	2 CONV 1 FC 2 OUT	tanh: conv sigm: FC sigm: L-FC	Local: 2 sub, 2 MI L/R hand, 460 trials/sub, 1000 Hz, 28 elec.	CV (10 folds)	86.4 ± 0.77	–	CM, PR, RC, F-score
Uktveris et al. 2017, [89]	ALL (22)	7-30	N/A	SI: SFI (FFT) [C × F]	CNN	2 CONV 1 FC 4 OUT	ReLU: conv Smax: L-FC	BCI-C IV-2a [131]	CV (10 folds)	68	–	–
Lu et al. 2016, [77]	ALL (3)	8-35	W	EF: FFT (also WPD)	DBN-RBM	3 RBM (1 hid) 1 FC 2 OUT	Smax: L-FC	BCI-C IV-2b [101]	HO (56 : 44)	84	–	t-test
Tabar et al. 2016, [98]	ALL (3)	6-30	W	SI: TFI (STEF) [T × F+C]	Hybrid: CNN/SAE (also, CNN, SAE)	1 CONV 6 AE (1 hid) 1 FC 2 OUT	ReLU: conv sigm: AE N/A: FC	DS1: BCI-C IV-2b [101] DS2: BCI-C II-3 [102]	DS1: CV (10 folds) DS2: HO (50 : 50)	DS1: 77.6 ± 2.1 DS2: 90.0	DS1: 0.55 DS2: 0.80	–

Pre-processing, *Selected channels*, ***ALL:*** *All dataset channels,* ***variable:*** *varying numbers of channels. Analyzed frequency band,* ***FB****: full-bandwidth in the dataset (0–frequency-end). Artifact removal approach,* ***W****: Without,* ***M****: Manual,* ***A****: Automatic [****ICA****: Independent component analysis,* ***DWT****: Discrete wavelet transform,* ***CAR****: Common average reference filter,* ***AAR****: Automatic artifact removal toolbox,* ***ASR****: Artifact subspace reconstruction,* ***BSS****: Blind source separation,* ***MRIC****: Movement related independent component,* ***SWT****: Synchrosqueezed wavelet transforms].*

Input formulation*, (* refer to Figure 10),* ***RV****: Raw values,* ***EF****: Extracted features [Frequency features [****FFT****: Fast Fourier transform,* ***DCT****: Discrete cosine transform,* ***PSD****: Power spectral density [****LSP****: Lomb-Scargle periodogram]], Time-frequency features [****EMD****: Empirical mode decomposition,* ***HHT****: Hilbert-Huang transform,* ***WT****: Wavelet transform,* ***DWT****: Discrete wavelet transform,* ***WPD****: Wavelet packet decomposition], Spatial features [****CSP****: Common spatial pattern,* ***FBCSP****: Filter bank CSP],* ***NSCM****: Normalized sample covariance matrix,* ***SM****: Statistical measures,* ***CorrM****: Correlation matrix,* ***PCA****: Principal component analysis],* ***SI****: Spectral images [****TFI****: Time-frequency images [****ST****: Stockwell transform,* ***QTFD****: Quadratic time-frequency distribution, WT [****CWT****: Continuous wavelet transform,* ***MW****: Morlet wavelets],* ***STFT****: Short-time Fourier transform],* ***SFI****: Spatial-frequency images],* ***TM****: Topological maps [****TP****: Time-domain point [****D****: Direct map,* ***G****: Graph-based],* ***SP****: Spectral-domain power].****T****: Time window (time segment),* ***TP****: Time point (sampling point),* ***F****: Frequency,* ***F-band****: Frequency band,* ***C****: Channel (electrode).*

Deep learning approaches, *General strategy, CNN, RNN [GRU, LSTM], MLP, RBM, AE, DBN [DBN-RBM, DBN-AE], ELM,* ***DSN****: Deep stacking network [DSN-RBM], GAN, VAE, Hybrid [CNN/LSTM, CNN/GRU, CNN/MLP, CNN/AE, CNN/VAE, CNN/GAN], SVM,* ***multi-layer****: multi-layer technique (for CNNs),* ***multi-branch****: multiple branches of CNNs (Ensemble learning),* ***augment****: data augmentation,* ***SW****: Sliding window,* ***NS****: Noise addition,* ***AP****: amplitude-perturbation. Architectures:* ***CONV****: Convolutional layer,* ***FC****: Fully connected layer,* ***DB****: Dense block,* ***LSTM-L:*** *LSTM layer****, GRU-L****: GRU layer,* ***hid****: hidden layer,* ***OUT****: number of (output) classes. Activation function,* ***ReLU****: Rectified linear unit,* ***LReLU****: Leaky rectified linear unit,* ***ELU****: Exponential linear unit,* ***SELU****: Scaled exponential linear unit,* ***tanh****: hyperbolic tangent,* ***sigm****: Sigmoid,* ***Smax****: Softmax function,* ***Linear****: Linear function,* ***L-FC****: Last fully connected layer,* ***G-conv, d-conv****: Convolution layer in a (generator/discriminant generator) model.*

Dataset, ***Local****: Private dataset (not available),* ***sub****: Subjects,* ***elec****: Electrode,* ***L/R****: left/right,* ***sess****: Session, "****x s trial****": Trial duration is x seconds.*

Evaluation Strategy, ***HO****: Hold-out (train: test),* ***CV****: Cross-validation,* ***LOSO****: leave-one-subject-out,* ***c-sub****: Cross-subject,* ***sub-d****: Subject-dependent,* ***sub-i****: Subject-independent,* ***CM****: Confusion matrix,* ***PR****: Precision (PPV),* ***RC****: Recall (True negative rate (TPR)/sensitivity),* ***TNR****: True negative rate (specificity),* ***ITR****: Information transfer rate,* ***ROC****: Receiver operating characteristic curve,* ***AUC****: Area under the curve,* ***T-comp****: Time complexity,* ***w-test****: Wilcoxon test, "****(x : y subs)****": x subjects for training and y subjects for testing.*

A visualization of the classification accuracy of EEG-based motor imagery (MI) reported by the latest deep learning-based articles for all public MI datasets.

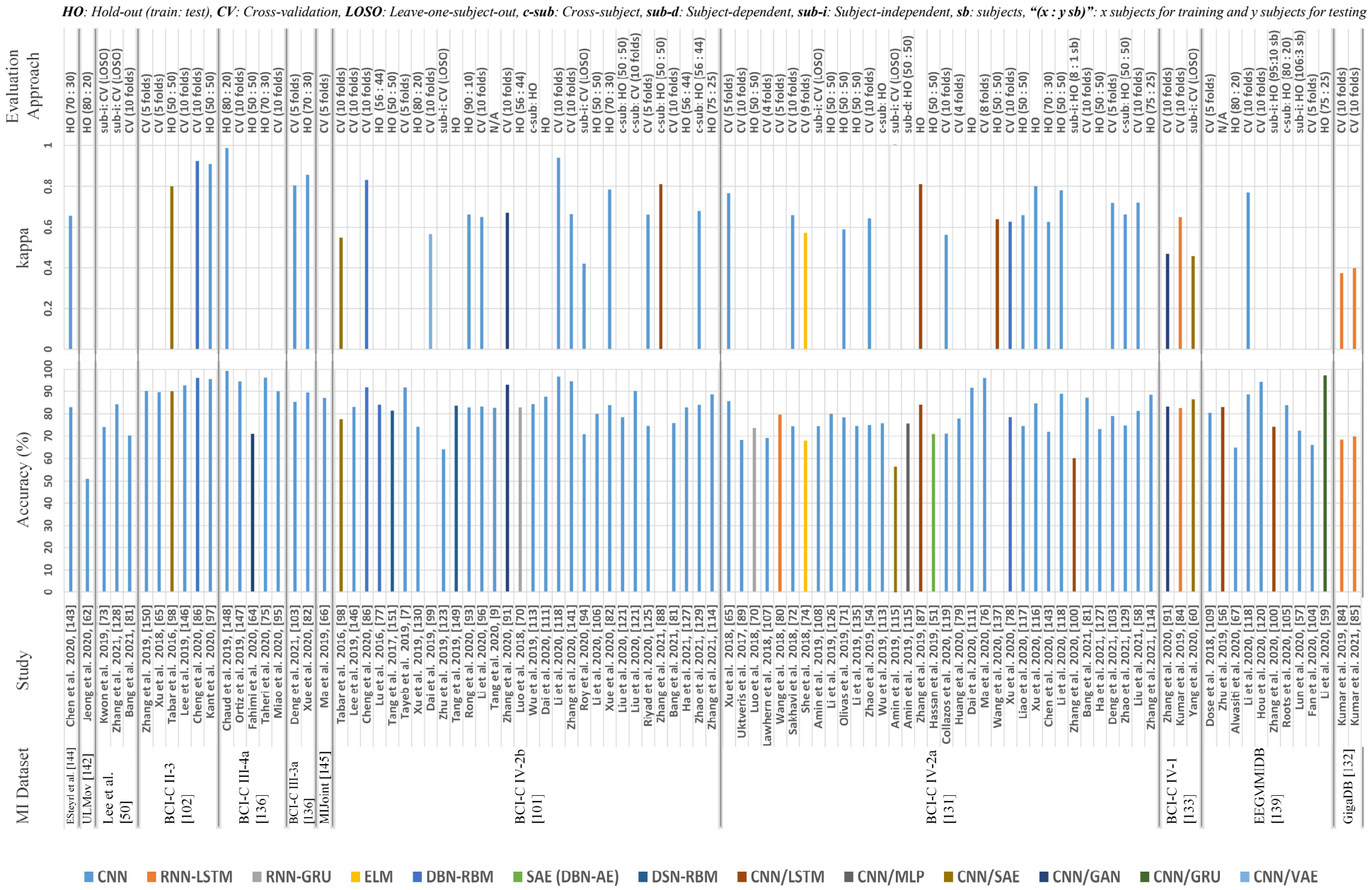

References

[1] F. Alshehri and G. Muhammad, "A comprehensive survey of the Internet of Things (IoT) and AI-based smart healthcare," *IEEE ACCESS*, vol. 9, pp. 3660–3678, 2021.

[2] M. Masud *et al.*, "A lightweight and robust secure key establishment protocol for internet of medical things in COVID-19 patients care," *IEEE Internet Things J.*, 2020.

[3] G. Muhammad, F. Alshehri, F. Karray, A. El Saddik, M. Alsulaiman, and T. H. Falk, "A comprehensive survey on multimodal medical signals fusion for smart healthcare systems," *Inf. Fusion*, 2021.

[4] J. Cantillo-Negrete, R. I. Carino-Escobar, P. Carrillo-Mora, D. Elias-Vinas, and J. Gutierrez-Martinez, "Motor imagery-based brain-computer interface coupled to a robotic hand orthosis aimed for neurorehabilitation of stroke patients," *J. Healthc. Eng.*, vol. 2018, 2018.

[5] E. López-Larraz, A. Sarasola-Sanz, N. Irastorza-Landa, N. Birbaumer, and A. Ramos-Murguialday, "Brain-machine interfaces for rehabilitation in stroke: A review," *NeuroRehabilitation*, vol. 43, no. 1, pp. 77–97, 2018.

[6] M. S. Al-Quraishi, I. Elamvazuthi, S. A. Daud, S. Parasuraman, and A. Borboni, "EEG-based control for upper and lower limb exoskeletons and prostheses: A systematic review," *Sensors*, vol. 18, no. 10, p. 3342, 2018.

[7] Z. Tayeb *et al.*, "Validating deep neural networks for online decoding of motor imagery movements from EEG signals," *Sensors*, vol. 19, no. 1, p. 210, 2019.

[8] Á. Fernández-Rodríguez, F. Velasco-Álvarez, and R. Ron-Angevin, "Review of real brain-controlled wheelchairs," *J. Neural Eng.*, vol. 13, no. 6, p. 61001, 2016.

[9] X. Tang, W. Li, X. Li, W. Ma, and X. Dang, "Motor imagery EEG recognition based on conditional optimization empirical mode decomposition and multi-scale convolutional neural network," *Expert Syst. Appl.*, vol. 149, p. 113285, 2020.

[10] J. Li, J. Liang, Q. Zhao, J. Li, K. Hong, and L. Zhang, "Design of assistive wheelchair system directly steered by human thoughts," *Int. J. Neural Syst.*, vol. 23, no. 03, p. 1350013, 2013.

[11] L. Cao, B. Xia, O. Maysam, J. Li, H. Xie, and N. Birbaumer, "A synchronous motor imagery based neural physiological paradigm for brain computer interface speller," *Front. Hum. Neurosci.*, vol. 11, p. 274, 2017.

[12] D. Das Chakladar and S. Chakraborty, "Multi-target way of cursor movement in brain computer interface using unsupervised learning," *Biol. Inspired Cogn. Archit.*, vol. 25, pp. 88–100, 2018.

[13] A. Delorme, T. Sejnowski, and S. Makeig, "Enhanced detection of artifacts in EEG data using higher-order statistics and independent component analysis," *Neuroimage*, vol. 34, no. 4, pp. 1443–1449, 2007.

[14] A. Jafarifarmand and M. A. Badamchizadeh, "EEG artifacts handling in a real practical brain–computer interface controlled vehicle," *IEEE Trans. Neural Syst. Rehabil. Eng.*, vol. 27, no. 6, pp. 1200–1208, 2019.

[15] D. Pawar and S. Dhage, "Feature Extraction Methods for Electroencephalography based Brain-Computer Interface: A Review.," *IAENG Int. J. Comput. Sci.*, vol. 47, no. 3, 2020.

[16] E. C. Djamal, M. Y. Abdullah, and F. Renaldi, "Brain computer interface game controlling using fast fourier transform and learning vector quantization," *J. Telecommun. Electron. Comput. Eng.*, vol. 9, no. 2–5, pp. 71–74, 2017.

[17] M. R. N. Kousarrizi, A. A. Ghanbari, M. Teshnehlab, M. A. Shorehdeli, and A. Gharaviri, "Feature extraction and classification of EEG signals using Wavelet transform, SVM and artificial neural networks for brain computer interfaces," in *2009 International Joint Conference on Bioinformatics, Systems Biology and Intelligent Computing*, 2009, pp. 352–355.

[18] L. Wang, Z. Lan, Q. Wang, R. Yang, and H. Li, "ELM_Kernel and Wavelet Packet Decomposition Based EEG Classification Algorithm," *Autom. Control Comput. Sci.*, vol. 53, no. 5, pp. 452–460, 2019.

[19] H. Ramoser, J. Muller-Gerking, and G. Pfurtscheller, "Optimal spatial filtering of single trial EEG during imagined hand movement," *IEEE Trans. Rehabil. Eng.*, vol. 8, no. 4, pp. 441–446, 2000.

[20] L. Zhang, D. Wen, C. Li, and R. Zhu, "Ensemble classifier based on optimized extreme learning machine for motor imagery classification," *J. Neural Eng.*, vol. 17, no. 2, p. 26004, 2020.

[21] K. Wang, D.-H. Zhai, and Y. Xia, "Motor Imagination EEG Recognition Algorithm based on DWT, CSP and Extreme Learning Machine," in *2019 Chinese Control Conference (CCC)*, 2019, pp. 4590–4595.

[22] Z. Jin, G. Zhou, D. Gao, and Y. Zhang, "EEG classification using sparse Bayesian extreme learning machine for brain–computer interface," *Neural Comput. Appl.*, pp. 1–9, 2018.

[23] K. K. Ang, Z. Y. Chin, C. Wang, C. Guan, and H. Zhang, "Filter bank common spatial pattern algorithm on BCI competition IV datasets 2a and 2b," *Front. Neurosci.*, vol. 6, p. 39, 2012.

[24] C.-Y. Chen, C.-W. Wu, C.-T. Lin, and S.-A. Chen, "A novel classification method for motor imagery based on Brain-Computer Interface," in *2014 International Joint Conference on Neural Networks (IJCNN)*, 2014, pp. 4099–4102.

[25] M. Arvaneh, C. Guan, K. K. Ang, and C. Quek, "Optimizing the channel selection and classification accuracy in EEG-based BCI," *IEEE Trans. Biomed. Eng.*, vol. 58, no. 6, pp. 1865–1873, 2011.

[26] W. Samek, C. Vidaurre, K.-R. Müller, and M. Kawanabe, "Stationary common spatial patterns for brain–computer interfacing," *J. Neural Eng.*, vol. 9, no. 2, p. 26013, 2012.

[27] W. Samek, M. Kawanabe, and K.-R. Müller, "Divergence-based framework for common spatial patterns algorithms," *IEEE Rev. Biomed. Eng.*, vol. 7, pp. 50–72, 2013.

[28] W. Wu, Z. Chen, X. Gao, Y. Li, E. N. Brown, and S. Gao, "Probabilistic common spatial patterns for multichannel EEG analysis," *IEEE Trans. Pattern Anal. Mach. Intell.*, vol. 37, no. 3, pp. 639–653, 2014.

[29] M. Rashid *et al.*, "Current Status, Challenges, and Possible Solutions of EEG-Based Brain-Computer Interface: A Comprehensive Review," *Front. Neurorobot.*, 2020.

[30] X. Zhang, L. Yao, X. Wang, J. J. M. Monaghan, D. Mcalpine, and Y. Zhang, "A survey on deep learning-based non-invasive brain signals: recent advances and new frontiers," *J. Neural Eng.*, 2020.

[31] H. Altaheri, M. Alsulaiman, and G. Muhammad, "Date Fruit Classification for Robotic Harvesting in a Natural Environment Using Deep Learning," *IEEE Access*, vol. 7, no. 1, pp. 117115–117133, Aug. 2019.

[32] M. Qamhan, H. Altaheri, A. H. Meftah, G. Muhammad, and Y. A. Alotaibi, "Digital Audio Forensics: Microphone and Environment Classification Using Deep Learning," *IEEE Access*, vol. 9, pp. 62719–62733, 2021.

[33] G. Muhammad, M. S. Hossain, and N. Kumar, "EEG-based pathology detection for home health monitoring," *IEEE J. Sel. Areas Commun.*, vol. 39, no. 2, pp. 603–610, 2020.

[34] G. Muhammad, M. F. Alhamid, and X. Long, "Computing and processing on the edge: Smart pathology detection for connected healthcare," *IEEE Netw.*, vol. 33, no. 6, pp. 44–49, 2019.

[35] G. Muhammad, S. K. M. M. Rahman, A. Alelaiwi, and A. Alamri, "Smart health solution integrating IoT and cloud: A case study of voice pathology monitoring," *IEEE Commun. Mag.*, vol. 55, no. 1, pp. 69–73, 2017.

[36] F. Lotte *et al.*, "A review of classification algorithms for EEG-based brain–computer interfaces: a 10 year update," *J. Neural Eng.*, vol. 15, no. 3, p. 31005, 2018.

[37] A. Craik, Y. He, and J. L. Contreras-Vidal, "Deep learning for electroencephalogram (EEG) classification tasks: a review," *J. Neural Eng.*, vol. 16, no. 3, p. 31001, 2019.

[38] N. Padfield, J. Zabalza, H. Zhao, V. Masero, and J. Ren, "EEG-based brain-computer interfaces using motor-imagery: Techniques and challenges," *Sensors*, vol. 19, no. 6, p. 1423, 2019.

[39] S. Aggarwal and N. Chugh, "Signal processing techniques for motor imagery brain computer interface: A review," *Array*, vol. 1, p. 100003, 2019.

[40] Z. Wan, R. Yang, M. Huang, N. Zeng, and X. Liu, "A review on transfer learning in EEG signal analysis," *Neurocomputing*, vol. 421, pp. 1–14, 2020.

[41] E. Lashgari, D. Liang, and U. Maoz, "Data augmentation for deep-learning-based electroencephalography," *J. Neurosci. Methods*, p. 108885, 2020.

[42] D. Moher, A. Liberati, J. Tetzlaff, D. G. Altman, and P. Group, "Preferred reporting items for systematic reviews and meta-analyses: the PRISMA statement," *PLoS med*, vol. 6, no. 7, p. e1000097, 2009.

[43] J. del R. Millán *et al.*, "Combining brain–computer interfaces and assistive technologies: state-of-the-art and challenges," *Front. Neurosci.*, vol. 4, p. 161, 2010.

[44] L. J. Greenfield, J. D. Geyer, and P. R. Carney, *Reading EEGs: A practical approach*. Lippincott Williams & Wilkins, 2012.

[45] T. Ball, M. Kern, I. Mutschler, A. Aertsen, and A. Schulze-

Bonhage, “Signal quality of simultaneously recorded invasive and non-invasive EEG,” *Neuroimage*, vol. 46, no. 3, pp. 708–716, 2009.
[46] E. R. Kandel, J. H. Schwartz, T. M. Jessell, S. Siegelbaum, A. J. Hudspeth, and S. Mack, *Principles of neural science*, vol. 4. McGraw-hill New York, 2000.
[47] “CHB-MIT Scalp EEG Database.” [Online]. Available: https://archive.physionet.org/physiobank/charts/chbmit.png. [Accessed: 12-Apr-2020].
[48] S. Lacey and R. Lawson, *Multisensory imagery*. Springer Science & Business Media, 2013.
[49] A. Rezeika, M. Benda, P. Stawicki, F. Gembler, A. Saboor, and I. Volosyak, “Brain–computer interface spellers: A review,” *Brain Sci.*, vol. 8, no. 4, p. 57, 2018.
[50] M.-H. Lee *et al.*, “EEG dataset and OpenBMI toolbox for three BCI paradigms: an investigation into BCI illiteracy,” *Gigascience*, vol. 8, no. 5, p. giz002, 2019.
[51] A. Hassanpour, M. Moradikia, H. Adeli, S. R. Khayami, and P. Shamsinejadbabaki, “A novel end-to-end deep learning scheme for classifying multi-class motor imagery electroencephalography signals,” *Expert Syst.*, vol. 36, no. 6, p. e12494, 2019.
[52] G. Pfurtscheller, C. Brunner, A. Schlögl, and F. H. L. Da Silva, “Mu rhythm (de) synchronization and EEG single-trial classification of different motor imagery tasks,” *Neuroimage*, vol. 31, no. 1, pp. 153–159, 2006.
[53] Y. Wang, M. Nakanishi, and D. Zhang, “EEG-Based Brain-Computer Interfaces,” in *Neural Interface: Frontiers and Applications*, Springer, 2019, pp. 41–65.
[54] X. Zhao, H. Zhang, G. Zhu, F. You, S. Kuang, and L. Sun, “A multi-branch 3D convolutional neural network for EEG-based motor imagery classification,” *IEEE Trans. Neural Syst. Rehabil. Eng.*, vol. 27, no. 10, pp. 2164–2177, 2019.
[55] O. Avilov, S. Rimbert, A. Popov, and L. Bougrain, “Optimizing Motor Intention Detection with Deep Learning: Towards Management of Intraoperative Awareness,” *IEEE Trans. Biomed. Eng.*, 2021.
[56] K. Zhu, S. Wang, D. Zheng, and M. Dai, “Study on the effect of different electrode channel combinations of motor imagery eeg signals on classification accuracy,” *J. Eng.*, vol. 2019, no. 23, pp. 8641–8645, 2019.
[57] X. Lun, Z. Yu, T. Chen, F. Wang, and Y. Hou, “A simplified CNN classification method for MI-EEG via the electrode pairs signals,” *Front. Hum. Neurosci.*, vol. 14, 2020.
[58] T. Liu and D. Yang, “A Densely Connected Multi-Branch 3D Convolutional Neural Network for Motor Imagery EEG Decoding,” *Brain Sci.*, vol. 11, no. 2, p. 197, 2021.
[59] Y. Li, H. Yang, J. Li, D. Chen, and M. Du, “EEG-based intention recognition with deep recurrent-convolution neural network: Performance and channel selection by Grad-CAM,” *Neurocomputing*, vol. 415, pp. 225–233, 2020.
[60] J. Yang, Z. Ma, J. Wang, and Y. Fu, “A Novel Deep Learning Scheme for Motor Imagery EEG Decoding Based on Spatial Representation Fusion,” *IEEE Access*, vol. 8, pp. 202100–202110, 2020.
[61] Y. Chu, X. Zhao, Y. Zou, W. Xu, J. Han, and Y. Zhao, “A decoding scheme for incomplete motor imagery EEG with deep belief network,” *Front. Neurosci.*, vol. 12, p. 680, 2018.
[62] J.-H. Jeong, B.-H. Lee, D.-H. Lee, Y.-D. Yun, and S.-W. Lee, “EEG classification of forearm movement imagery using a hierarchical flow convolutional neural network,” *IEEE Access*, vol. 8, pp. 66941–66950, 2020.
[63] J. Yang, S. Yao, and J. Wang, “Deep fusion feature learning network for MI-EEG classification,” *IEEE Access*, vol. 6, pp. 79050–79059, 2018.
[64] F. Fahimi, S. Dosen, K. K. Ang, N. Mrachacz-Kersting, and C. Guan, “Generative Adversarial Networks-Based Data Augmentation for Brain-Computer Interface,” *IEEE Trans. neural networks Learn. Syst.*, 2020.
[65] B. Xu *et al.*, “Wavelet transform time-frequency image and convolutional network-based motor imagery EEG classification,” *IEEE Access*, vol. 7, pp. 6084–6093, 2018.
[66] X. Ma, S. Qiu, W. Wei, S. Wang, and H. He, “Deep Channel-Correlation Network for Motor Imagery Decoding From the Same Limb,” *IEEE Trans. Neural Syst. Rehabil. Eng.*, vol. 28, no. 1, pp. 297–306, 2019.
[67] H. Alwasiti, M. Z. Yusoff, and K. Raza, “Motor imagery classification for brain computer interface using deep metric learning,” *IEEE Access*, vol. 8, pp. 109949–109963, 2020.
[68] R. Alazrai, M. Abuhijleh, H. Alwanni, and M. I. Daoud, “A deep learning framework for decoding motor imagery tasks of the same hand using eeg signals,” *IEEE Access*, vol. 7, pp. 109612–109627, 2019.
[69] G. Gómez-Herrero *et al.*, “Automatic removal of ocular artifacts in the EEG without an EOG reference channel,” in *Proceedings of the 7th Nordic Signal Processing Symposium-NORSIG 2006*, 2006, pp. 130–133.
[70] T. Luo and F. Chao, “Exploring spatial-frequency-sequential relationships for motor imagery classification with recurrent neural network,” *BMC Bioinformatics*, vol. 19, no. 1, p. 344, 2018.
[71] B. E. Olivas-Padilla and M. I. Chacon-Murguia, “Classification of multiple motor imagery using deep convolutional neural networks and spatial filters,” *Appl. Soft Comput.*, vol. 75, pp. 461–472, 2019.
[72] S. Sakhavi, C. Guan, and S. Yan, “Learning temporal information for brain-computer interface using convolutional neural networks,” *IEEE Trans. neural networks Learn. Syst.*, vol. 29, no. 11, pp. 5619–5629, 2018.
[73] O.-Y. Kwon, M.-H. Lee, C. Guan, and S.-W. Lee, “Subject-independent brain–computer interfaces based on deep convolutional neural networks,” *IEEE Trans. neural networks Learn. Syst.*, vol. 31, no. 10, pp. 3839–3852, 2019.
[74] Q. She, B. Hu, Z. Luo, T. Nguyen, and Y. Zhang, “A hierarchical semi-supervised extreme learning machine method for EEG recognition,” *Med. Biol. Eng. Comput.*, vol. 57, no. 1, pp. 147–157, 2018.
[75] S. Taheri, M. Ezoji, and S. M. Sakhaei, “Convolutional neural network based features for motor imagery EEG signals classification in brain–computer interface system,” *SN Appl. Sci.*, vol. 2, no. 4, pp. 1–12, 2020.
[76] X. Ma, D. Wang, D. Liu, and J. Yang, “DWT and CNN based multi-class motor imagery electroencephalographic signal recognition,” *J. Neural Eng.*, vol. 17, no. 1, p. 16073, 2020.
[77] N. Lu, T. Li, X. Ren, and H. Miao, “A deep learning scheme for motor imagery classification based on restricted Boltzmann machines,” *IEEE Trans. neural Syst. Rehabil. Eng.*, vol. 25, no. 6, pp. 566–576, 2016.
[78] J. Xu, H. Zheng, J. Wang, D. Li, and X. Fang, “Recognition of EEG signal motor imagery intention based on deep multi-view feature learning,” *Sensors*, vol. 20, no. 12, p. 3496, 2020.
[79] W. Huang, Y. Xue, L. Hu, and H. Liuli, “S-EEGNet: Electroencephalogram Signal Classification Based on a Separable Convolution Neural Network With Bilinear Interpolation,” *IEEE Access*, vol. 8, pp. 131636–131646, 2020.
[80] P. Wang, A. Jiang, X. Liu, J. Shang, and L. Zhang, “LSTM-based EEG classification in motor imagery tasks,” *IEEE Trans. neural Syst. Rehabil. Eng.*, vol. 26, no. 11, pp. 2086–2095, 2018.
[81] J.-S. Bang, M.-H. Lee, S. Fazli, C. Guan, and S.-W. Lee, “Spatio-spectral feature representation for motor imagery classification using convolutional neural networks,” *IEEE Trans. Neural Networks Learn. Syst.*, 2021.
[82] J. Xue *et al.*, “A Multifrequency Brain Network-Based Deep Learning Framework for Motor Imagery Decoding,” *Neural Plast.*, vol. 2020, 2020.
[83] X. Zhao, J. Zhao, C. Liu, and W. Cai, “Deep neural network with joint distribution matching for cross-subject motor imagery brain-computer interfaces,” *Biomed Res. Int.*, vol. 2020, 2020.
[84] S. Kumar, A. Sharma, and T. Tsunoda, “Brain wave classification using long short-term memory network based OPTICAL predictor,” *Sci. Rep.*, vol. 9, no. 1, pp. 1–13, 2019.
[85] S. Kumar, R. Sharma, and A. Sharma, “OPTICAL+: a frequency-based deep learning scheme for recognizing brain wave signals,” *PeerJ Comput. Sci.*, vol. 7, p. e375, 2021.
[86] L. Cheng, D. Li, G. Yu, Z. Zhang, X. Li, and S. Yu, “A Motor Imagery EEG Feature Extraction Method Based on Energy Principal Component Analysis and Deep Belief Networks,” *IEEE Access*, vol. 8, pp. 21453–21472, 2020.
[87] R. Zhang, Q. Zong, L. Dou, and X. Zhao, “A novel hybrid deep learning scheme for four-class motor imagery classification,” *J. Neural Eng.*, vol. 16, no. 6, p. 66004, 2019.
[88] R. Zhang, Q. Zong, L. Dou, X. Zhao, Y. Tang, and Z. Li, “Hybrid deep neural network using transfer learning for EEG motor imagery decoding,” *Biomed. Signal Process. Control*, vol. 63, p. 102144, 2021.
[89] T. Uktveris and V. Jusas, “Application of convolutional neural networks to four-class motor imagery classification problem,” *Inf. Technol. Control*, vol. 46, no. 2, pp. 260–273, 2017.
[90] Z. Wang, L. Cao, Z. Zhang, X. Gong, Y. Sun, and H. Wang, “Short time Fourier transformation and deep neural networks for motor

imagery brain computer interface recognition," *Concurr. Comput. Pract. Exp.*, vol. 30, no. 23, p. e4413, 2018.
[91] K. Zhang *et al.*, "Data augmentation for motor imagery signal classification based on a hybrid neural network," *Sensors*, vol. 20, no. 16, p. 4485, 2020.
[92] N. Shajil, S. Mohan, P. Srinivasan, J. Arivudaiyanambi, and A. A. Murrugesan, "Multiclass Classification of Spatially Filtered Motor Imagery EEG Signals Using Convolutional Neural Network for BCI Based Applications," *J. Med. Biol. Eng.*, vol. 40, no. 5, pp. 663–672, 2020.
[93] Y. Rong, X. Wu, and Y. Zhang, "Classification of motor imagery electroencephalography signals using continuous small convolutional neural network," *Int. J. Imaging Syst. Technol.*, vol. 30, no. 3, pp. 653–659, 2020.
[94] S. Roy, A. Chowdhury, K. McCreadie, and G. Prasad, "Deep learning based inter-subject continuous decoding of motor imagery for practical brain-computer interfaces," *Front. Neurosci.*, vol. 14, 2020.
[95] M. Miao, W. Hu, H. Yin, and K. Zhang, "Spatial-frequency feature learning and classification of motor imagery EEG based on deep convolution neural network," *Comput. Math. Methods Med.*, vol. 2020, 2020.
[96] F. Li, F. He, F. Wang, D. Zhang, Y. Xia, and X. Li, "A novel simplified convolutional neural network classification algorithm of motor imagery EEG signals based on deep learning," *Appl. Sci.*, vol. 10, no. 5, p. 1605, 2020.
[97] P. Kant, S. H. Laskar, J. Hazarika, and R. Mahamune, "CWT Based Transfer Learning for Motor Imagery Classification for Brain computer Interfaces," *J. Neurosci. Methods*, vol. 345, p. 108886, 2020.
[98] Y. R. Tabar and U. Halici, "A novel deep learning approach for classification of EEG motor imagery signals," *J. Neural Eng.*, vol. 14, no. 1, p. 16003, 2016.
[99] M. Dai, D. Zheng, R. Na, S. Wang, and S. Zhang, "EEG classification of motor imagery using a novel deep learning framework," *Sensors*, vol. 19, no. 3, p. 551, 2019.
[100] D. Zhang, K. Chen, D. Jian, and L. Yao, "Motor imagery classification via temporal attention cues of graph embedded EEG signals," *IEEE J. Biomed. Heal. informatics*, vol. 24, no. 9, pp. 2570–2579, 2020.
[101] R. Leeb, C. Brunner, G. Müller-Putz, A. Schlögl, and G. Pfurtscheller, "BCI Competition 2008–Graz data set B," *Inst. Knowl. Discov. Graz Univ. Technol.*, pp. 1–6, 2008.
[102] B. Blankertz *et al.*, "The BCI competition 2003: progress and perspectives in detection and discrimination of EEG single trials," *IEEE Trans. Biomed. Eng.*, vol. 51, no. 6, pp. 1044–1051, 2004.
[103] X. Deng, B. Zhang, N. Yu, K. Liu, and K. Sun, "Advanced TSGL-EEGNet for Motor Imagery EEG-Based Brain-Computer Interfaces," *IEEE Access*, vol. 9, pp. 25118–25130, 2021.
[104] C.-C. Fan, H. Yang, Z.-G. Hou, Z.-L. Ni, S. Chen, and Z. Fang, "Bilinear neural network with 3-D attention for brain decoding of motor imagery movements from the human EEG," *Cogn. Neurodyn.*, vol. 15, no. 1, pp. 181–189, 2021.
[105] K. Roots, Y. Muhammad, and N. Muhammad, "Fusion Convolutional Neural Network for Cross-Subject EEG Motor Imagery Classification," *Computers*, vol. 9, no. 3, p. 72, 2020.
[106] D. Li, J. Xu, J. Wang, X. Fang, and J. Ying, "A Multi-Scale Fusion Convolutional Neural Network based on Attention Mechanism for the Visualization Analysis of EEG Signals Decoding," *IEEE Trans. Neural Syst. Rehabil. Eng.*, 2020.
[107] V. J. Lawhern, A. J. Solon, N. R. Waytowich, S. M. Gordon, C. P. Hung, and B. J. Lance, "EEGNet: a compact convolutional neural network for EEG-based brain–computer interfaces," *J. Neural Eng.*, vol. 15, no. 5, p. 56013, 2018.
[108] S. U. Amin, M. Alsulaiman, G. Muhammad, M. A. Bencherif, and M. S. Hossain, "Multilevel weighted feature fusion using convolutional neural networks for EEG motor imagery classification," *IEEE Access*, vol. 7, pp. 18940–18950, 2019.
[109] H. Dose, J. S. Møller, H. K. Iversen, and S. Puthusserypady, "An end-to-end deep learning approach to MI-EEG signal classification for BCIs," *Expert Syst. Appl.*, vol. 114, pp. 532–542, 2018.
[110] Z. Tang, C. Li, and S. Sun, "Single-trial EEG classification of motor imagery using deep convolutional neural networks," *Optik (Stuttg).*, vol. 130, pp. 11–18, 2017.
[111] G. Dai, J. Zhou, J. Huang, and N. Wang, "HS-CNN: a CNN with hybrid convolution scale for EEG motor imagery classification," *J. Neural Eng.*, vol. 17, no. 1, p. 16025, 2020.
[112] B.-H. Lee, J.-H. Jeong, and S.-W. Lee, "SessionNet: Feature similarity-based weighted ensemble learning for motor imagery classification," *IEEE Access*, vol. 8, pp. 134524–134535, 2020.
[113] H. Wu *et al.*, "A Parallel Multiscale Filter Bank Convolutional Neural Networks for Motor Imagery EEG Classification," *Front. Neurosci.*, vol. 13, p. 1275, 2019.
[114] C. Zhang, Y.-K. Kim, and A. Eskandarian, "EEG-inception: an accurate and robust end-to-end neural network for EEG-based motor imagery classification," *J. Neural Eng.*, vol. 18, no. 4, p. 46014, 2021.
[115] S. U. Amin, M. Alsulaiman, G. Muhammad, M. A. Mekhtiche, and M. S. Hossain, "Deep Learning for EEG motor imagery classification based on multi-layer CNNs feature fusion," *Futur. Gener. Comput. Syst.*, vol. 101, pp. 542–554, 2019.
[116] M. Xu *et al.*, "Learning EEG topographical representation for classification via convolutional neural network," *Pattern Recognit.*, vol. 105, p. 107390, 2020.
[117] J. J. Liao, J. J. Luo, T. Yang, R. Q. Y. So, and M. C. H. Chua, "Effects of local and global spatial patterns in EEG motor-imagery classification using convolutional neural network," *Brain-Computer Interfaces*, vol. 7, no. 3–4, pp. 47–56, 2020.
[118] M.-A. Li, J.-F. Han, and L.-J. Duan, "A Novel MI-EEG Imaging With the Location Information of Electrodes," *IEEE Access*, vol. 8, pp. 3197–3211, 2019.
[119] D. F. Collazos-Huertas, A. M. Álvarez-Meza, C. D. Acosta-Medina, G. A. Castaño-Duque, and G. Castellanos-Dominguez, "CNN-based framework using spatial dropping for enhanced interpretation of neural activity in motor imagery classification," *Brain Informatics*, vol. 7, no. 1, pp. 1–13, 2020.
[120] Y. Hou, L. Zhou, S. Jia, and X. Lun, "A novel approach of decoding EEG four-class motor imagery tasks via scout ESI and CNN," *J. Neural Eng.*, vol. 17, no. 1, p. 16048, 2020.
[121] X. Liu, Y. Shen, J. Liu, J. Yang, P. Xiong, and F. Lin, "Parallel Spatial–Temporal Self-Attention CNN-Based Motor Imagery Classification for BCI," *Front. Neurosci.*, vol. 14, 2020.
[122] S. U. Amin, H. Altaheri, G. Muhammad, M. Alsulaiman, and W. Abdul, "Attention based Inception model for robust EEG motor imagery classification," in *2021 IEEE International Instrumentation and Measurement Technology Conference (I2MTC)*, 2021, pp. 1–6.
[123] X. Zhu, P. Li, C. Li, D. Yao, R. Zhang, and P. Xu, "Separated channel convolutional neural network to realize the training free motor imagery BCI systems," *Biomed. Signal Process. Control*, vol. 49, pp. 396–403, 2019.
[124] Y. K. Musallam *et al.*, "Electroencephalography-based motor imagery classification using temporal convolutional network fusion," *Biomed. Signal Process. Control*, vol. 69, p. 102826, 2021.
[125] M. Riyad, M. Khalil, and A. Adib, "MI-EEGNET: A novel convolutional neural network for motor imagery classification," *J. Neurosci. Methods*, vol. 353, p. 109037, 2021.
[126] D. Li, J. Wang, J. Xu, and X. Fang, "Densely feature fusion based on convolutional neural networks for motor imagery EEG classification," *IEEE Access*, vol. 7, pp. 132720–132730, 2019.
[127] K.-W. Ha and J.-W. Jeong, "Temporal Pyramid Pooling for Decoding Motor-Imagery EEG Signals," *IEEE Access*, vol. 9, pp. 3112–3125, 2021.
[128] K. Zhang, N. Robinson, S.-W. Lee, and C. Guan, "Adaptive transfer learning for EEG motor imagery classification with deep Convolutional Neural Network," *Neural Networks*, vol. 136, pp. 1–10, 2021.
[129] H. Zhao, Q. Zheng, K. Ma, H. Li, and Y. Zheng, "Deep Representation-Based Domain Adaptation for Nonstationary EEG Classification," *IEEE Trans. Neural Networks Learn. Syst.*, 2020.
[130] G. Xu *et al.*, "A deep transfer convolutional neural network framework for EEG signal classification," *IEEE Access*, vol. 7, pp. 112767–112776, 2019.
[131] C. Brunner, R. Leeb, G. Müller-Putz, A. Schlögl, and G. Pfurtscheller, "BCI Competition 2008–Graz data set A," *Inst. Knowl. Discov. Graz Univ. Technol.*, vol. 16, pp. 1–6, 2008.
[132] H. Cho, M. Ahn, S. Ahn, M. Kwon, and S. C. Jun, "EEG datasets for motor imagery brain–computer interface," *Gigascience*, vol. 6, no. 7, p. gix034, 2017.
[133] B. Blankertz, G. Dornhege, M. Krauledat, K.-R. Müller, and G. Curio, "The non-invasive Berlin brain–computer interface: fast acquisition of effective performance in untrained subjects," *Neuroimage*, vol. 37, no. 2, pp. 539–550, 2007.
[134] D. P. Kingma and M. Welling, "Auto-encoding variational bayes," *arXiv Prepr. arXiv1312.6114*, 2013.
[135] Y. Li, X.-R. Zhang, B. Zhang, M.-Y. Lei, W.-G. Cui, and Y.-Z.

Guo, “A channel-projection mixed-scale convolutional neural network for motor imagery EEG decoding,” *IEEE Trans. Neural Syst. Rehabil. Eng.*, vol. 27, no. 6, pp. 1170–1180, 2019.
[136] B. Blankertz *et al.*, “The BCI competition III: Validating alternative approaches to actual BCI problems,” *IEEE Trans. neural Syst. Rehabil. Eng.*, vol. 14, no. 2, pp. 153–159, 2006.
[137] L. Wang, W. Huang, Z. Yang, and C. Zhang, “Temporal-spatial-frequency depth extraction of brain-computer interface based on mental tasks,” *Biomed. Signal Process. Control*, vol. 58, p. 101845, 2020.
[138] D. Freer and G.-Z. Yang, “Data augmentation for self-paced motor imagery classification with C-LSTM,” *J. Neural Eng.*, vol. 17, no. 1, p. 16041, 2020.
[139] A. L. Goldberger *et al.*, “PhysioBank, PhysioToolkit, and PhysioNet: components of a new research resource for complex physiologic signals,” *Circulation*, vol. 101, no. 23, pp. e215–e220, 2000.
[140] L. Xiaoling, “Motor imagery-based EEG signals classification by combining temporal and spatial deep characteristics,” *Int. J. Intell. Comput. Cybern.*, 2020.
[141] K. Zhang *et al.*, “Instance transfer subject-dependent strategy for motor imagery signal classification using deep convolutional neural networks,” *Comput. Math. Methods Med.*, vol. 2020, 2020.
[142] P. Ofner, A. Schwarz, J. Pereira, and G. R. Müller-Putz, “Upper limb movements can be decoded from the time-domain of low-frequency EEG,” *PLoS One*, vol. 12, no. 8, p. e0182578, 2017.
[143] J. Chen, Z. Yu, Z. Gu, and Y. Li, “Deep Temporal-Spatial Feature Learning for Motor Imagery-Based Brain–Computer Interfaces,” *IEEE Trans. Neural Syst. Rehabil. Eng.*, vol. 28, no. 11, pp. 2356–2366, 2020.
[144] D. Steyrl, R. Scherer, O. Förstner, and G. R. Müller-Putz, “Motor imagery brain-computer interfaces: random forests vs regularized LDA-non-linear beats linear,” in *Proceedings of the 6th International Brain-Computer Interface Conference*, 2014, pp. 241–244.
[145] X. Ma, S. Qiu, and H. He, “Multi-channel EEG recording during motor imagery of different joints from the same limb,” *Sci. data*, vol. 7, no. 1, pp. 1–9, 2020.
[146] H. K. Lee and Y.-S. Choi, “Application of continuous wavelet transform and convolutional neural network in decoding motor imagery brain-computer interface,” *Entropy*, vol. 21, no. 12, p. 1199, 2019.
[147] C. J. Ortiz-Echeverri, S. Salazar-Colores, J. Rodríguez-Reséndiz, and R. A. Gómez-Loenzo, “A new approach for motor imagery classification based on sorted blind source separation, continuous wavelet transform, and convolutional neural network,” *Sensors*, vol. 19, no. 20, p. 4541, 2019.
[148] S. Chaudhary, S. Taran, V. Bajaj, and A. Sengur, “Convolutional neural network based approach towards motor imagery tasks EEG signals classification,” *IEEE Sens. J.*, vol. 19, no. 12, pp. 4494–4500, 2019.
[149] X.-L. Tang, W.-C. Ma, D.-S. Kong, and W. Li, “Semisupervised deep stacking network with adaptive learning rate strategy for motor imagery EEG recognition,” *Neural Comput.*, vol. 31, no. 5, pp. 919–942, 2019.
[150] Z. Zhang *et al.*, “A novel deep learning approach with data augmentation to classify motor imagery signals,” *IEEE Access*, vol. 7, pp. 15945–15954, 2019.
[151] X. Tang, N. Zhang, J. Zhou, and Q. Liu, “Hidden-layer visible deep stacking network optimized by PSO for motor imagery EEG recognition,” *Neurocomputing*, vol. 234, pp. 1–10, 2017.
[152] L. Deng, Jia and Dong, Wei and Socher, Richard and Li, Li-Jia and Li, Kai and Fei-Fei, “Imagenet: A large-scale hierarchical image database,” in *IEEE Conference on Computer Vision and Pattern Recognition*, 2009, pp. 248–255.
[153] H. Altaheri, M. Alsulaiman, G. Muhammad, S. U. Amin, M. Bencherif, and M. Mekhtiche, “Date fruit dataset for intelligent harvesting,” *Data Br.*, vol. 26, p. 104514, Oct. 2019.
[154] M. Alsulaiman, G. Muhammad, M. A. Bencherif, A. Mahmood, and Z. Ali, “KSU rich Arabic speech database,” *Inf.*, vol. 16, no. 6 B, pp. 4231–4253, 2013.
[155] Graz University of Technology, “Data sets - BNCI Horizon 2020.” [Online]. Available: http://bnci-horizon-2020.eu/database/data-sets. [Accessed: 05-Feb-2021].
[156] F. Lotte, “Fabien Lotte’s professional homepage - Links.” [Online]. Available: https://sites.google.com/site/fabienlotte/bci-community/links?authuser=0#h.p_ID_172. [Accessed: 05-Feb-2021].
[157] R. Scherer *et al.*, “Individually adapted imagery improves brain-computer interface performance in end-users with disability,” *PLoS One*, vol. 10, no. 5, p. e0123727, 2015.
[158] M. Kaya, M. K. Binli, E. Ozbay, H. Yanar, and Y. Mishchenko, “A large electroencephalographic motor imagery dataset for electroencephalographic brain computer interfaces,” *Sci. data*, vol. 5, p. 180211, 2018.
[159] N. Brodu, F. Lotte, and A. Lécuyer, “Exploring two novel features for EEG-based brain–computer interfaces: Multifractal cumulants and predictive complexity,” *Neurocomputing*, vol. 79, pp. 87–94, 2012.
[160] A. Ramos-Murguialday *et al.*, “Brain–machine interface in chronic stroke rehabilitation: a controlled study,” *Ann. Neurol.*, vol. 74, no. 1, pp. 100–108, 2013.
[161] X. Zhang, L. Yao, Q. Z. Sheng, S. S. Kanhere, T. Gu, and D. Zhang, “Converting your thoughts to texts: Enabling brain typing via deep feature learning of eeg signals,” in *2018 IEEE international conference on pervasive computing and communications (PerCom)*, 2018, pp. 1–10.
[162] J. Van Erp, F. Lotte, and M. Tangermann, “Brain-computer interfaces: beyond medical applications,” *Computer (Long. Beach. Calif).*, vol. 45, no. 4, pp. 26–34, 2012.
[163] R. Yuste *et al.*, “Four ethical priorities for neurotechnologies and AI,” *Nat. News*, vol. 551, no. 7679, p. 159, 2017.
[164] K. LaFleur, K. Cassady, A. Doud, K. Shades, E. Rogin, and B. He, “Quadcopter control in three-dimensional space using a noninvasive motor imagery-based brain–computer interface,” *J. Neural Eng.*, vol. 10, no. 4, p. 46003, 2013.
[165] Y. Yu *et al.*, “Toward brain-actuated car applications: Self-paced control with a motor imagery-based brain-computer interface,” *Comput. Biol. Med.*, vol. 77, pp. 148–155, 2016.
[166] X. Zhang, L. Yao, C. Huang, Q. Z. Sheng, and X. Wang, “Intent recognition in smart living through deep recurrent neural networks,” in *International Conference on Neural Information Processing*, 2017, pp. 748–758.
[167] T. Li, J. Zhang, T. Xue, and B. Wang, “Development of a novel motor imagery control technique and application in a gaming environment,” *Comput. Intell. Neurosci.*, vol. 2017, 2017.
[168] A. Kreilinger, H. Hiebel, and G. R. Müller-Putz, “Single versus multiple events error potential detection in a BCI-controlled car game with continuous and discrete feedback,” *IEEE Trans. Biomed. Eng.*, vol. 63, no. 3, pp. 519–529, 2015.
[169] X. Zhang, L. Yao, S. S. Kanhere, Y. Liu, T. Gu, and K. Chen, “Mindid: Person identification from brain waves through attention-based recurrent neural network,” *Proc. ACM Interactive, Mobile, Wearable Ubiquitous Technol.*, vol. 2, no. 3, pp. 1–23, 2018.
[170] X. Zhang, L. Yao, C. Huang, T. Gu, Z. Yang, and Y. Liu, “DeepKey: An EEG and gait based dual-authentication system,” *arXiv Prepr. arXiv1706.01606*, 2017.